Fermi National Accelerator Laboratory

FERMILAB-Conf-99/282-E
CDF

CDF Results on Hard Diffraction and Rapidity Gap Physics

M. Convery
For the CDF Collaboration

The Rockefeller University
1230 York Avenue, New York, New York 10021

Fermi National Accelerator Laboratory
P.O. Box 500, Batavia, Illinois 60510

October 1999

Published Proceedings of the *19th International Symposium on Multiparticle Dynamics (ISMD99)*, Providence, Rhode Island, August 9-13, 1999

Operated by Universities Research Association Inc. under Contract No. DE-AC02-76CH03000 with the United States Department of Energy

Disclaimer

This report was prepared as an account of work sponsored by an agency of the United States Government. Neither the United States Government nor any agency thereof, nor any of their employees, makes any warranty, expressed or implied, or assumes any legal liability or responsibility for the accuracy, completeness, or usefulness of any information, apparatus, product, or process disclosed, or represents that its use would not infringe privately owned rights. Reference herein to any specific commercial product, process, or service by trade name, trademark, manufacturer, or otherwise, does not necessarily constitute or imply its endorsement, recommendation, or favoring by the United States Government or any agency thereof. The views and opinions of authors expressed herein do not necessarily state or reflect those of the United States Government or any agency thereof.

Distribution

Approved for public release; further dissemination unlimited.

Copyright Notification

CDF RESULTS ON HARD DIFFRACTION AND RAPIDITY GAP PHYSICS

M. E. CONVERY
The Rockefeller University, 1230 York Avenue, New York, NY 10021, USA
E-mail: convery@fnal.gov

We review published rapidity gap results on diffractive W and dijet production and discuss new results on diffractive b and J/ψ production. The diffractive structure function of the proton obtained from Roman pot dijet data is presented and compared with expectations based on the diffractive parton densities extracted from DIS at HERA. Also presented are results on dijet production in double Pomeron exchange. Finally, we review hard double-diffractive results (rapidity gaps between jets) and present new results on soft double diffraction.

1 Introduction

We report on results obtained by CDF at the Fermilab Tevatron $\bar{p}p$ collider at $\sqrt{s} = 1800$ GeV. Much work has been done recently to study the nature of diffractive interactions, and comparisons of ep collisions at HERA with Tevatron results are necessary to test our understanding. The CDF collaboration has studied hard single and double diffraction and double Pomeron exchange, illustrated in Fig. 1, by detecting rapidity gaps, regions devoid of particles, and forward $\bar{p}$'s using Roman-pot detectors. We have also studied soft double diffraction and made comparisons of the measured cross sections to predictions from Regge theory.

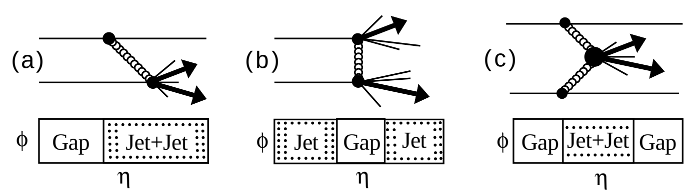

Figure 1: Dijet production in hard (a) single- and (b) double-diffractive scattering and in (c) double-Pomeron-exchange interactions.

The CDF detector has calorimeters covering the region $|\eta| < 4.2$. Charged tracks are detected in the region $|\eta| < 1.1$, inside a 1.5 T solenoid magnetic field. The parts of the detector most relevant for the diffractive analyses are the forward calorimeters, which cover $2.4 < |\eta| < 4.2$, the beam-beam counters (BBC's) consisting of scintillator covering the region $3.2 < |\eta| < 5.9$, which can be used to trigger on beam-beam collisions, and the three Roman pot detectors located approximately 57 m downstream in the antiproton direction.

2 Rapidity gaps in hard single diffraction

Hard single diffraction has previously been studied by CDF in events with rapidity gaps corresponding to Pomeron momentum fraction $\xi < 0.1$ in W and dijet production. The ratio of single-diffractive (SD) to non-diffractive (ND) W production was found to be [1]

$$R_W = [1.15 \pm 0.51(stat) \pm 0.20(syst)]\%.$$

The fraction of events with dijets in the range $E_T^{jet} > 20$ GeV, $1.8 < |\eta^{jet}| < 3.5$ and $\eta^{jet1}\eta^{jet2} > 0$ produced diffractively was determined to be [2]

$$R_{GJJ} = [0.75 \pm 0.05(stat) \pm 0.09(syst)]\%.$$

Since diffractive W production is mostly sensitive to quarks in the Pomeron, while dijet production is mainly sensitive to gluons, these two measurements can be combined to determine the gluon fraction in the Pomeron, $f_g = 0.7 \pm 0.2$. This is consistent with the fraction found by the ZEUS collaboration. The rate of hard-diffractive production was found to be lower than expectations based on diffractive structure functions determined at HERA by a discrepancy factor of $D = 0.18 \pm 0.04$.

The diffractive signal was observed in these events as a rapidity gap (no particles observed) in both the forward calorimeter (FCAL) and the BBC on one side of the detector, the side opposite the jets in dijet events. In the histogram of FCAL ($E_T \geq 1.5$ GeV) and BBC multiplicity shown in Fig. 2 for events with a b quark, the gap events can be seen as a peak in the (0,0) bin. The ND background in the (0,0) bin is determined by plotting the number of events in the diagonal bins, those in which the same number of hits are observed in the FCAL and BBC, and fitting a straight line to the bins corresponding to non-zero multiplicity. This line is then extrapolated to give the background in the zero bin. The background-subtracted rapidity gap events in the (0,0) bin must then be corrected for gap acceptance, since not all SD events with $\xi < 0.1$ will be found in the (0,0) bin. The fraction of b quarks which are produced diffractively is found to be [3]

$$R_{\bar{b}b} = [0.62 \pm 0.19(stat) \pm 0.16(syst)]\%.$$

Combining the results from diffractive b quark production with the W and dijet results as shown in Fig. 3 give a gluon fraction in the Pomeron of

$$f_g = 0.54^{+0.16}_{-0.14}.$$

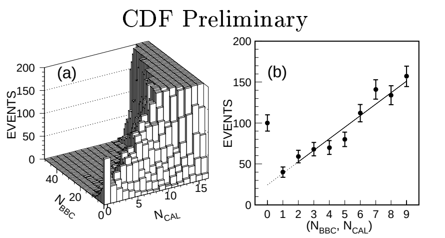

Figure 2: (a) Beam-beam counter multiplicity N_{BBC} versus forward calorimeter tower multiplicity N_{CAL}; (b) multiplicity distribution along the diagonal with $N_{BBC} = N_{CAL}$ in the plot in (a).

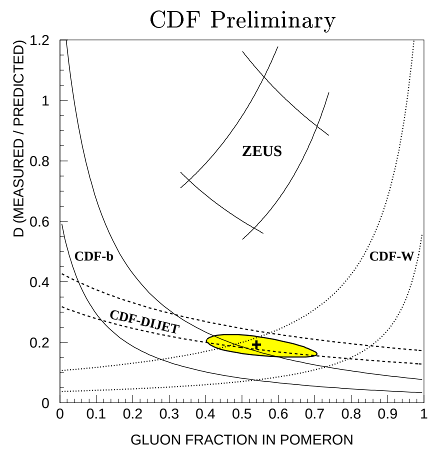

Figure 3: The ratio, D, of measured to predicted diffractive rates as a function of the gluon content of the Pomeron. The black cross and shaded ellipse are the best fit and 1σ contour of a least square two-parameter fit to the three CDF results.

Preliminary results for J/ψ production, before correcting for the gap acceptance A, give a SD/ND ratio of

$$R_{J/\psi} \times A = [0.64 \pm 0.10(stat)]\%.$$

Although the different processes studied in rapidity gap events have different sensitivities to quarks and gluons in the Pomeron, SD/ND ratios are found to be of similar magnitude, $\sim 1\%$, for all processes. This suggests that the structure of the Pomeron probed in SD events is not very different than the structure of the proton probed in ND events.

3 Study of diffractive structure functions in dijet events using Roman pots

Single-diffractive dijet events were also studied using the Roman pot detectors to detect diffractive $\bar{p}$'s, which carry away a fraction x of their original momentum. The fraction of the momentum taken by the Pomeron is $\xi = 1 - x$, and the fraction of the Pomeron momentum carried by the parton which is involved in the hard scattering, β, is given by $x_{\bar{p}} = \beta\xi$.

In the region $0.035 < \xi < 0.095$ and $-t \leq 1.0$ GeV^2, the fraction of events with a Roman-pot track which have dijets of $E_T > 7$ GeV increases with increasing ξ. The leading jet E_T distributions fall faster with E_T in the SD than in the ND events. This is due to the difference in SD and ND structure functions which are discussed below. The SD dijets are boosted away from the leading $\bar{p}$ in η, and are more back-to-back in ϕ than ND dijets. In the region $0 < |t| < 3$ GeV^2, the ratio of dijet to inclusive SD events is found to be independent of t.

The goal of these studies is to measure the structure, using dijet production, of the interacting $\bar{p}$ in events with a $\bar{p}$ detected in the Roman pot detectors, and compare it with the structure in ND events. The $x_{\bar{p}}$ is determined from the jets (including a third jet if $E_T^{jet3} > 5$ GeV) as $x_{\bar{p}} = \sum_{i=1,2(3)} E_T^i e^{-\eta_i}/(2p_0^{\bar{p}})$. The ratio of SD to ND dijet cross sections as a function of $x_{\bar{p}}$, determined by correctly normalizing the number of SD and ND events observed, is equivalent to the ratio of the SD to ND $\bar{p}$ structure functions. Note that this ratio of the $\bar{p}$ structure functions in events with and without a rapidity gap is determined independently of any Monte Carlo simulations, and does not depend on the concept of a Pomeron.

This ratio R is shown in Fig. 4 as a function of $x_{\bar{p}}$ for six bins in ξ of width 0.01 ranging from 0.035 to 0.095 for $x_{\bar{p}} > 10^{-3}$. These distributions, plotted on a log-log axis of R vs. $x_{\bar{p}}$, are well fit by lines in the region $x_{\bar{p}} < 0.5\,\langle\xi\rangle$ with similar slopes for all ξ bins. A fit combining all ξ bins yields $R \propto 1/x_{\bar{p}}^{0.46}$.

The ND structure function F_{JJ} and SD structure function F_{JJ}^D can be written in terms of quark and gluon densities with appropriate color factors as $F_{JJ}^{(D)}(x_{\bar{p}}) = x_{\bar{p}}\{g^{(D)}(x_{\bar{p}}) + \frac{4}{9}\sum_i[q_i^{(D)}(x_{\bar{p}}) + \bar{q}_i^{(D)}(x_{\bar{p}})]\}$. The SD structure function can be determined from the measured ratio and the known ND structure function, and compared to the SD structure function found using the "fit 2" and "fit 3" parton densities determined by the H1 collaboration at HERA. First we change variables to $\beta = x_{\bar{p}}/\xi$. Figure 5 shows F_{JJ}^D as a function of β and the fit $F_{JJ}^D \propto 1/\beta^{1.04}$ (solid line). The dashed (dotted) lines are obtained from fit 2 (fit 3) of the H1 parton densities, scaled down by a factor of 20. We find that the shape of fit 3 does not agree with CDF data at large β. A comparison of the CDF data to fit 2 shows good agreement in shape in the region well measured by H1, $\beta >\sim 0.3$. Summed over all β, the rate of diffractive dijet production observed at CDF is about a factor of 10 lower than at H1, in general agreement with renormalized flux model predictions.[4]

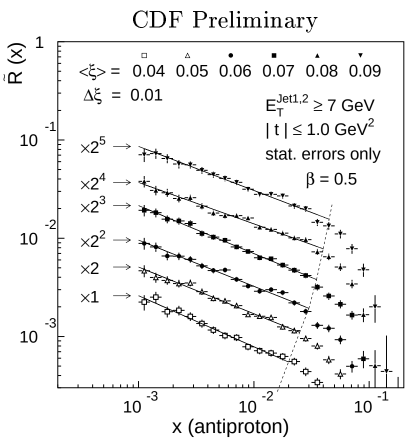

Figure 4: Ratio of diffractive to non-diffractive dijet event rates as a function of x (momentum fraction of parton in $\bar{p}$). The solid lines are fits to the form $R(x) = R_0 x^{-r}$ for $\beta(= x/\xi) < 0.5$.

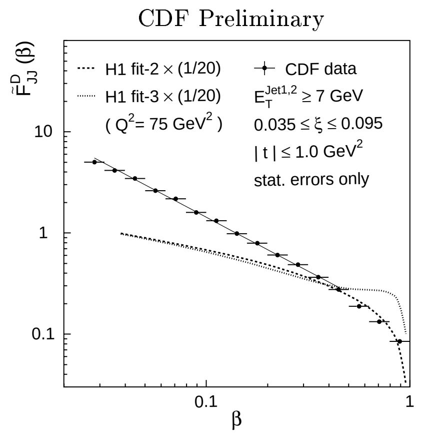

Figure 5: The β distribution from the data (points) and fit (solid line), compared with expectations from the diffractive parton densities of the proton from H1 fit 2 (dashed) and fit 3 (dotted) scaled down by a factor of 20.

4 Double Pomeron exchange

As shown in Fig. 1, in hard double-Pomeron-exchange (DPE) interactions, dijets are produced in the central region, separated from the diffractive p and $\bar{p}$ by forward rapidity gaps. DPE events have been studied at CDF using the Roman pots to detect the $\bar{p}$, and requiring a rapidity gap in the FCAL and BBC on the p side in the same way as was done in SD rapidity gap studies. Preliminary results give the fraction of events with dijets of $E_T > 7$ GeV and a Roman pot track which also have a gap on the proton side of

$$R_{DPE/SD} = [0.40 \pm 0.04(\text{stat}) \pm 0.08(\text{syst})]\%.$$

Recall that the rate of SD dijet production was found to be $\sim 1\%$ of the ND rate. In double-diffractive dijet production (discussed below), where there is also only one rapidity gap, the fraction of events with dijets with $\eta_1\eta_2 < 0$ produced diffractively is also $\sim 1\%$. The DPE dijet events, which have two rapidity gaps, are found at a rate which is another factor of 1% or so lower.

Studies of factorization are under way to determine if differences in DPE/SD and SD/ND comparisons are due to purely kinematical effects of the additional gap, and therefore lower effective $\sqrt{s}$, or if factorization breaks down.

5 Hard and soft double diffraction

Double-diffractive (DD) events are characterized by the exchange of a color singlet with the quantum numbers of the vacuum, the Pomeron, causing both incident hadrons to dissociate (Fig. 1). The dissociated hadrons produce diffractive mass clusters along their initial direction, while, since the exchanged object does not radiate as, for example, a colored object would, the region in between the clusters is empty of particles.

Hard double diffraction has previously been studied in events with rapidity gaps between jets. The fraction of dijet events with $1.8 < |\eta^{jet1,jet2}| < 3.5$, $\eta^{jet1}\eta^{jet2} < 0$, and $E_T^{jet1,jet2} > 20$ GeV at $\sqrt{s} = 1800$ GeV due to color singlet exchange (CSE) was found to be [5]

$$R_{JGJ}(1800) = [1.13 \pm 0.12(stat) \pm 0.11(syst)]\%,$$

and for jets with $E_T^{jet1,jet2} > 8$ GeV at $\sqrt{s} = 630$ GeV [6]

$$R_{JGJ}(630) = [2.7 \pm 0.7(stat) \pm 0.6(syst)]\%,$$

so that the CSE fraction at 630 GeV is greater than that at 1800 GeV by a factor of

$$R(630)/R(1800) = 2.4 \pm 0.7(stat) \pm 0.6(syst).$$

The distribution of the CSE fraction as a function of the rapidity separation between the jets was seen to drop as the jets reached the edges of the acceptance. No dependence was observed of the CSE fraction on mean dijet E_T or on jet x, determined from the E_T and η of the jets as $x_i = e^{|\eta_i|}E_T^i/\sqrt{s}$.

We have studied soft double diffraction by looking for central rapidity gaps in minimum-bias events which have hits in the BBC's. We looked for gaps which overlap $\eta = 0$ rather than the largest gap anywhere in the detector because the latter method is more likely to be biased by inefficiencies in the calorimeters. The η of the track or calorimeter tower above a given threshold with the smallest $|\eta|$ for $\eta > 0$ ($\eta < 0$) is defined to be $\eta_{max(min)}$, as shown in Fig. 6. Figure 7 compares the data to ND, SD, and DD Monte Carlo (MC) simulated events as a function of η_{max} and $-\eta_{min}$. Structure due to different thresholds and efficiencies in the calorimeter can be seen, e.g., at the interface between the plug and forward calorimeters at $\eta \sim 2.4$. The bins for $|\eta_{max(min)}| > 3.2$ contain all events with the lowest-$|\eta|$ particle in the BBC, $3.2 < |\eta| < 5.9$.

The SD contribution is fixed by known cross sections and the fraction of events passing the BBC trigger in the MC. The ND and DD contributions are determined as follows. Figure 8 shows the number of events in the data

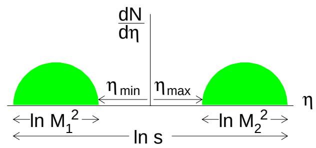

Figure 6: A double-diffractive interaction at center-of-mass energy $\sqrt{s}$, producing diffractive masses M_1 and M_2 separated by a rapidity gap of width $\eta_{max} - \eta_{min}$.

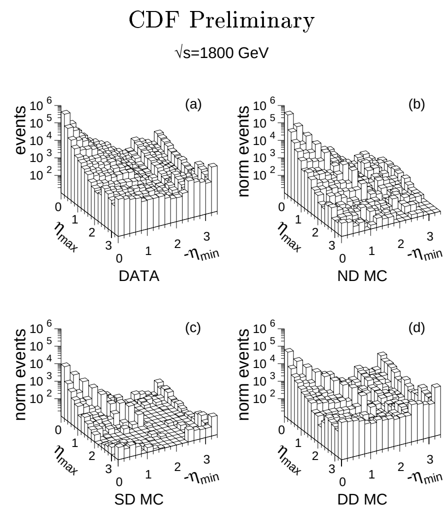

Figure 7: The number of events as a function of η_{max} and $-\eta_{min}$: (a) 1800 GeV data, (b) ND, (c) SD and (d) DD MC-generated events.

and MC as a function of $\Delta\eta^0 = \eta_{max} - \eta_{min}$. The DD and non-DD MC distributions are normalized to give the number of events observed in the data in the region $\Delta\eta^0 < 0.8$ (dominantly ND) and $\Delta\eta^0 > 3$ (dominantly DD). The DD MC uses the differential cross sections from Regge theory based on the triple Pomeron amplitude and factorization. The agreement between data and MC seen in Fig. 8 shows that Regge theory appears to correctly predict the mass dependence, as was also observed by the H1 collaboration. [7] Note that the fluctuations in the $\Delta\eta^0$ distribution are due to structure in the calorimeter and are followed closely by the MC because of careful calibrations derived to match MC particle p_T's to observed calorimeter E_T's.

We find cross sections at $\sqrt{s} = 1800$ (630) GeV by measuring $\sigma_{DD}\mathcal{A}$, where $\mathcal{A}$ is the acceptance of triggering on diffractive mass clusters. Preliminary calculations from MC yield $\mathcal{A} = (48.7 \pm 8.4)\%$ $[(61.4 \pm 6.8)\%]$, and

$$\sigma_{DD}(\sqrt{s} = 1800 \text{ GeV}, \Delta\eta^0 > 3) = 4.71 \pm 0.02(stat)^{+0.92}_{-0.90}(syst) \text{ mb},$$

$$\sigma_{DD}(\sqrt{s} = 630 \text{ GeV}, \Delta\eta^0 > 3) = 4.32 \pm 0.01(stat)^{+0.54}_{-0.76}(syst) \text{ mb}.$$

The cross sections for all gaps of width $\Delta y > 2.3$, corresponding to the SD coherence limit of $\xi < 0.1$, can be obtained by extrapolation using the differential cross section shape from Regge theory, and are greater by a factor of 1.72 (1.67) at $\sqrt{s} = 1800$ (630) GeV. The resulting cross sections are shown in Fig. 9 along with results from UA5 [8] and other cross sections at lower energies, [9,10] most of which were derived from exclusive measurements using factorization relations. The DD cross sections measured by CDF are an order of magnitude smaller than what is predicted using Regge theory, but are in general agreement with the renormalized gap model. [11]

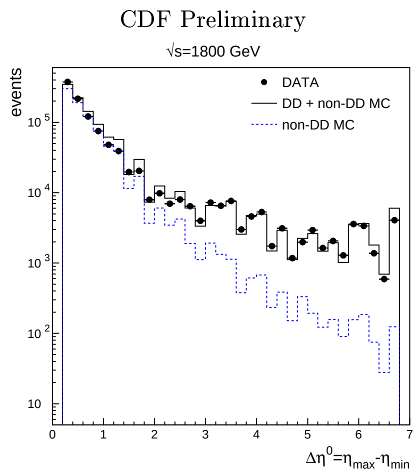

Figure 8: The number of events as a function of $\Delta\eta^0 = \eta_{max} - \eta_{min}$ for 1800 GeV data, and for DD + non-DD and only non-DD MC-generated events.

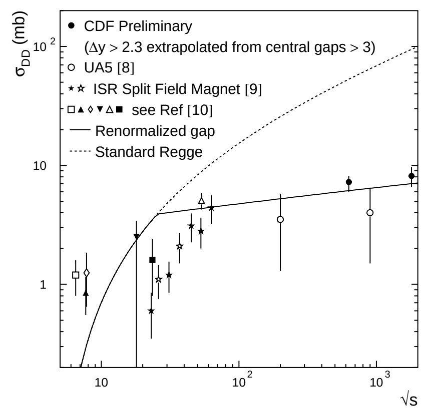

Figure 9: The total DD cross section versus $\sqrt{s}$ compared with predictions from standard Regge theory based on the triple-Pomeron amplitude and factorization (dashed curve) and from the renormalized gap model (solid curve).

References

1. F. Abe *et al.*, (CDF Collaboration), *Phys. Rev. Lett.* **78**, 2698 (1997).
2. F. Abe *et al.*, (CDF Collaboration), *Phys. Rev. Lett.* **79**, 2636 (1997).
3. T. Affolder *et al.*, (CDF Collaboration), submitted to Phys. Rev. Lett.
4. K. Goulianos, *Nucl. Phys. Proc. Suppl.* **71**, 368 (1999).
5. F. Abe *et al.*, (CDF Collaboration), *Phys. Rev. Lett.* **80**, 1156 (1998).
6. F. Abe *et al.*, (CDF Collaboration), *Phys. Rev. Lett.* **81**, 5278 (1998).
7. C. Adloff *et al.*, (H1 Collaboration), *Z. Phys.* C **74**, 221 (1997).
8. R. E. Ansorge *et al.*, (UA5 Collaboration), *Z. Phys.* C **33**, 175 (1986).
9. C. Conta *et al.*, *Nucl. Phys.* B **175**, 97 (1980).
10. A. Givernaud *et al.*, *Nucl. Phys.* B **152**, 189 (1979) and references therein.
11. K. Goulianos, *Phys. Lett.* B **358**, 379 (1995).